International Journal of Coal Science & Technology (2022) 9:26
https://doi.org/10.1007/s40789-022-00496-y

RESEARCH

Optically powered gas monitoring system using single-mode fibre for underground coal mines

Yingge Chen[1] · Leonardo Silvestri[1] · Xinyue Lei[1] · François Ladouceur[1]

Received: 7 June 2021 / Accepted: 2 April 2022

Abstract
We present an optically powered, intrinsically safe gas monitoring system to measure four essential environmental gases (CH_4, CO_2, CO and O_2), together with ambient temperature and pressure, for underground mines. The system is based on three key technologies developed at UNSW: (1) power-over-fibre (PoF) at 1550 nm using a single industry-standard, low-cost single-mode fibre (SMF) for both power delivery and information transmission, (2) liquid–crystal-based optical transducers for optical telemetry, and (3) ultra-low power consumption design of all electronics. Together, this approach allows each gas monitoring station to operate with less than 150 mW of optical power, meeting the intrinsic safety requirements specified by the IEC60079-28 standard. A 2-month field trial at BMA's Broadmeadow underground mine proved the cabling compatibility to the mine's existing optical network and the stability of the system performance. Compared with conventional electrically powered gas sensors, this technology bypasses the usual roadblocks of underground gas monitoring where electrical power is either unsafe or unavailable. Furthermore, using one fibre for both power delivery and communication enables longer distance coverage, reduces optical cabling and increases multiplexing possibilities and data throughput for better awareness of underground environment.

Keywords Power-over-fibre · Ultra-low power consumption · Gas monitoring · Intrinsic safety · Single-mode fibre · Optical transducer

1 Introduction

Continuous monitoring of mine atmosphere is essential for the safety, health and productivity of a mine. The presence of gases like CH_4, CO_2, CO and O_2 are relevant indicators of safety risks and gas monitoring systems recording the corresponding values and trends are required especially in the most hazardous zones like return airway and long-wall face (AS/NZS 2290.3 2018; Wasilewski and Jamóz 2018). Some mine sites after closure also require on-going monitoring of the residual hazards (U.S. Environmental Protection Agency 2014; Palchik 2014). In these remote and harsh areas, electrical power delivery is not always safe nor stable, and sometimes not available. Existing gas sensors are normally powered electrically via physical connections and require an uninterruptible power supply (UPS) in case of power shortage. The increasing number of installed sensors thus raises the risk of sparks and drives up the costs of installation and cable management (Einicke et al. 2011).

As many of the sensors in harsh environment use optical link for data transmission, and many modern mines have rolled out optical fibre networks, it would be desirable if both power and data could be transmitted optically thus eliminating copper wires (Werthen et al. 2005).

Power-over-fibre (PoF) technology has been applied to power electronics in many applications where the optical power transmitted via optical fibre is converted into electrical power by photovoltaic cells to provide power supply to the sensor. Early application of PoF dated back to 1978 when 5.95 mW optical power was used to power a telephone sound alerter (DeLoach et al. 1978). In 1995, PoF was introduced for gas monitoring in underground coal mine using 5 W light source before the establishment of explosion hazardous standard for fibre-optic equipment (Dubaniewicz and Chilton 1995). The technology has been further applied to other industries such as

✉ Yingge Chen
yingge.chen@unsw.edu.au

[1] School of Electrical Engineering and Telecommunications, University of New South Wales, Sydney, NSW 2052, Australia

Published online: 26 April 2022

telecommunication (Vázquez et al. 2019; Wake et al. 2008; Xu et al. 2010) and electric utilities, where high voltage and high current sensors are powered and read optically (Heinig et al. 2020; Bassan et al. 2021). Other low power consumption industrial sensors such as temperature sensor (Budelmann 2018), pressure sensor and proximity sensor (López-Cardona et al. 2018) using PoF technologies have demonstrated significant advantages over their electrical counterparts.

So far, in order to transmit enough power to the sensor, these PoF applications have been using multi-mode fibre (MMF) with large numerical aperture which limits the transmission distance and where one or two separate optical fibres are required for data transmission (Rosolem 2017).

For the applications in underground coal mine or other harsh environment, where intrinsic safety is required, these approaches have their limitations: (1) intrinsic safety standard (IEC 60079-28 2015) imposes strict limit on optical power delivered to a hazardous zone (e.g. 150 mW for underground coal mines), (2) long distance transmission is required to monitor previously unreachable area (e.g. from surface to an underground tailgate), (3) functions of certain sensors must be maintained (AS/NZS 2290.3 2018), e.g. local display, touch pad and visual alarm for gas sensors, which requires additional power.

We address these shortcomings by proposing and developing an intrinsically safe optically powered gas monitoring network based on (1) power-over-fibre (PoF) at 1550 nm using a single industry-standard, low cost single-mode fibre (SMF) for both power delivery and information transmission, (2) liquid–crystal-based optical transducers for optical telemetry, and (3) ultra-low power consumption design of the electronics and data transmission approach which allows each gas monitoring station of the sensing network to operate with less than 150 mW optical power, meeting the intrinsic safety requirement for optical radiation (IEC 60079-28 2015). This study was part of a two-year (2019–2020) ACARP program (C28010) aimed to tackle gas monitoring issues in underground coal mine tailgate return airway. In the following sections, we will discuss the principle of operation, the development and setup of the system, field trials and data analysis.

2 Principle of operation

2.1 Power-over-fibre

The PoF system proposed is illustrated in Fig. 1 and consists of a remote terminal unit (RTU) and one or more optically powered sensors connected by one single-mode fibre (SMF) for both power delivery and information transmission.

Inside the RTU, a 1550 nm amplified spontaneous emission (ASE) light source provides light through an optical circulator to the optically powered sensor which can be located kilometres away in the hazardous area. Inside the sensor, light is split by an optical coupler at a selected ratio (e.g. 99:1), with most of the power going to a photovoltaic converter and the rest to an optical transducer. The photovoltaic converter converts the optical power into electrical power to support the sensing and conditioning electronics, which incorporates low power analog to digital converters (ADCs) and a microcontroller to transform the analog signal from the sensor's sensing element into a digital signal with the desired characteristics.

The optical transducer converts the electrical signal from sensor electronics into an optical signal passively and reflects the signal back via the same optical path to the RTU. At the circulator, the optical signal is directed into the photodetector module where the optical signal is converted back into electrical signal. The data acquisition (DAQ) module then processes the signal and provides an Ethernet interface for users to monitor the measurement and conditions of the sensor in real time on a webpage.

2.2 Optical transducers

The optical transducers area based on liquid crystal (LC) cells that act as variable reflectance mirrors when coupled with a polariser (Brodzeli et al. 2013a). They convert

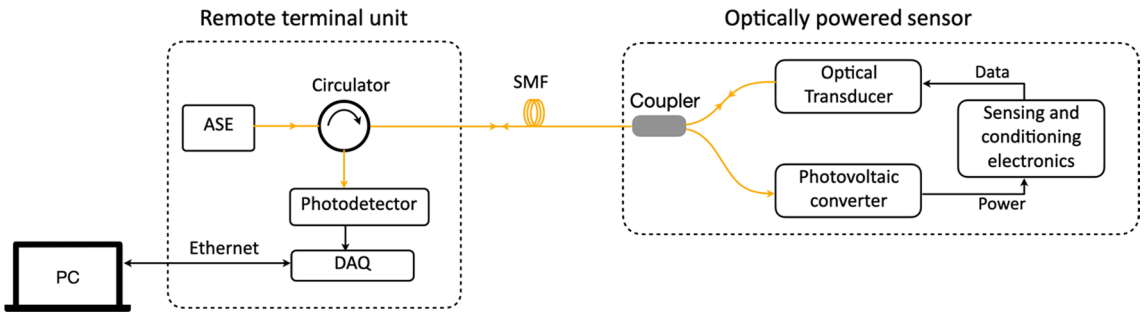

Fig. 1 Block diagram of the approach taken to implement power-over-fibre

electrical signals into optical signals without requiring any electrical power. Essentially, the cell consists of two substrates with conductive inner surfaces acting as electrodes, sandwiching a thin layer of liquid crystal (see Fig. 2). The liquid crystal layer is aligned with respect to the polariser in such a way as to induce a linear optical response to the input voltage. Deformed Helix Ferroelectric LC's are unique in their combination of fast switching speed (approximately 200 µs response time), and low driving voltage (Brodzeli et al. 2013b). The substrates are made of borosilicate glass, each with a transparent conductive film of indium tin oxide (ITO), and a gold mirror is attached to the back of the bottom substrate. The infrared light is delivered to the cell by single mode optical fibre. The light then passes through a polariser, the top substrate and the LC layer before undergoing reflection off the back surface of the cell.

In its simplest form, the two conductive substrates, each attached to a metal pin, are then connected to the output of the sensor whose signal drives the optical transducer such that the voltage across the LC cell causes the LC to modulate the reflected light being coupled back into the fibre. The modulated light intensity represents the sensor's signal which can then be transmitted via optical fibre. Applications of the optical transducers have proved that they reduce the power consumption of sensors by simplifying electronics and introduce advantages of optical telemetry such as covering long distance, immunity to EMI and ease of multiplexing (Firth et al. 2016, 2017; Lei et al. 2020).

2.3 Ultra-low power consumption design

As designed, each gas monitoring station incorporates four gas sensor cells, temperature and pressure sensors, and supports local display and digital communication. In order to power the station respecting an optical power budget of less than 150 mW, the power consumption of the device must be minimised ideally without performance trade-off. Three approaches have been taken to realise ultra-low power consumption.

(1) Use of low power components.

The low power microcontroller ATSAML21J18B is used to provide power management technologies, such as power domain gating, SleepWalking and Ultra-low-power peripherals. A Low Quiescent Current Low Drop Out voltage regulator (MCP1700T-3002E/MBCT-ND) is selected to optimise the power from the photovoltaic converter. Low power analog measurement circuitry is designed to read analog signals from sensor cells and touchpad at a very low power cost.

(2) Low power firmware design.

For most sensors, power consumption peaks upon their start-up. To limit peak power consumption, the firmware controls the warm-up sequence of individual sensor cells during power-up. The ATSAML21J17B micro-controller state-machine staggers this warm-up process so as not to over-load the optically sourced power supply. After warm- up, the micro-controller is running a state machine to select the sensor cells in sequence every 120 ms. After each cell is energised, sampled and de-energised the micro-controller is put to sleep to minimise current consumption.

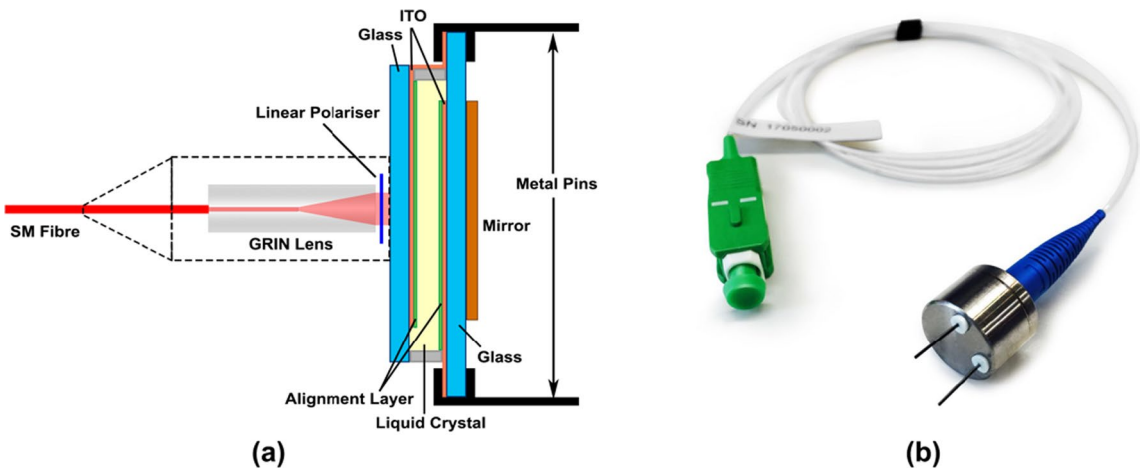

Fig. 2 Diagram showing the architecture of a typical liquid crystal (LC) transducer cell and packaged transducer with two electrical inputs (signal) and a single mode fibre input/output

(3) Communication with Manchester encoding.

We use Manchester encoding for its simplicity and self-synchronisation feature, and implement it in an energy efficient way. Manchester encoding uses the transition of voltage level rather than voltage level to represent the ones and zeros of any binary information, combining clock and data in one channel, making a synchronisation clock unnecessary. One-way communication from the sensor to the RTU further saves power as no information is received and processed inside the sensor. The Manchester modulating clock rate we use is 8 kHz, resulting 1 bit every 125 µs. Each Manchester packet takes 20 ms to transmit and it is transmitted every 120 ms. As a result, most of the time within every 120 ms, no data is transmitted and sensors are put to sleep by the firmware control, consuming energy only when necessary. The update rate for each sensor is 1.2 s, sufficient for real-time environmental monitoring.

3 Development of gas monitoring network

3.1 Gas monitoring station

Based on the PoF approach illustrated in Fig. 1, an optically powered gas monitoring station has been designed to measure CH_4, CO_2, CO and O_2, as well as ambient temperature and barometric pressure in one device. The block diagram and assembly of the gas monitoring station are shown in Fig. 3.

In Fig. 3a, the sensor signal conditioning module incorporates four gas sensor cells and a single sensor for

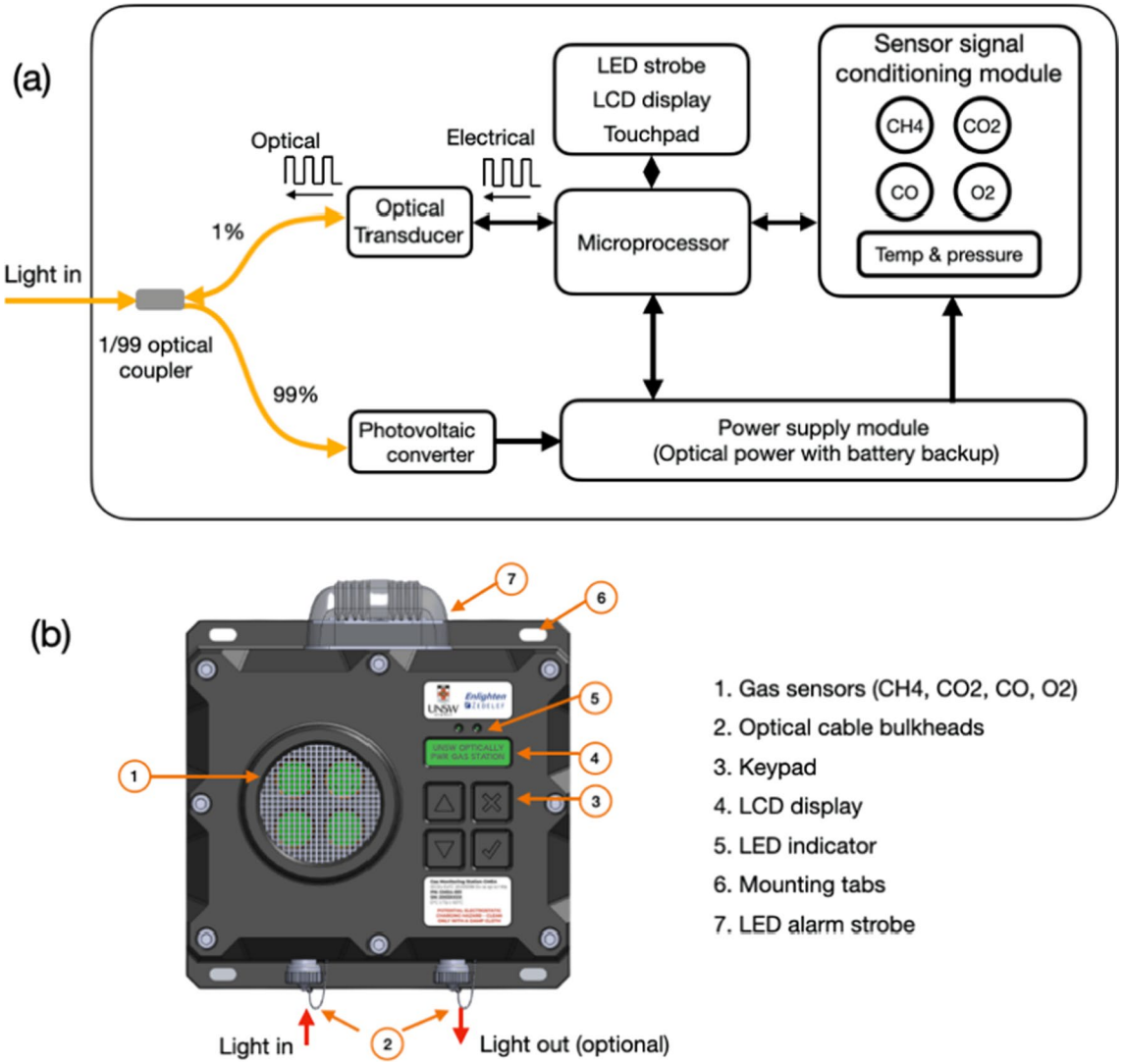

Fig. 3 Optically powered gas monitoring station. **a** Block diagram, and **b** Assembly and part names. Note how having both optical in- and out-ports allows to daisy chain a number of stations

temperature and pressure. CH_4 (MIPEX-02-1-II-1.1A) and CO_2 (MIPEX-02-3-II-1.1A) sensors are infrared gas sensors cells while O_2 (O2-A2) and CO (CO-A4) sensor cells are electrochemical. BMP280 digital pressure sensor is used to measure both ambient temperature and barometric pressure.

The conditioned sensing signals are then processed by an ultra-low-power microprocessor ATSAML21J18B which orchestrates all other actions from LCD display, touchpad, intrinsically safe LED strobe, power supply module, etc., into a Manchester encoded digital signal. The optical transducer receiving 1% of the incoming light converts the digital signal passively into an optical signal to be transmitted back to the RTU. All the electronics is powered by the power supply module and its circuit is designed in compliance with intrinsic safety standards (IEC 60079-0 2017; IEC 60079-11 2011).

The power supply module consists of a photovoltaic converter (KPC8-T) for 1300–1600 nm laser light as the main power source, a backup battery and its charge pump. 99% of the incoming light goes into the photovoltaic converter and is converted into a typical maximum voltage of 3.6 V at a power conversion efficiency around 30% to power the whole device through a voltage regulator. A 3.6 V battery (LS14500) is used as a backup power for temporary optical power failure and to power the LED strobe when/if triggered. When the supply voltage from the optical power is lower than 2.5 V, the battery will switch in and power the device via the charge pump circuit (instead of relying on optical power). Every minute the power supply condition is monitored, and as soon as the optical power is restored, it will replace the battery to power the device.

There are four modes of operation: 1) Warm-up mode, (2) Normal mode, (3) Alarm mode, and (4) Calibration mode.

When the gas monitoring station is turned on, it will start with a 60 s Warm-up mode. During the Warm-up mode, the powering of each sensor cell is sequenced to "level" the start-up power before the station enters Normal mode. The gas concentration thresholds can be set for 'low' and 'high' alarms for each gas sensor. When any alarm is triggered, the station will go into Alarm mode and the LED strobe goes off. In-situ calibration is supported allowing user to apply Zero and Span gas during which the device enters Calibration mode to avoid any false alarm caused by calibration gases. Information under each operation mode can be accessed both locally and remotely as light carrying the information back to the RTU enables real-time remote monitoring.

Based on this design, we fabricated two PCBs for each station. One dealing mainly with the optoelectronics while the second plays a more traditional role. The two are connected and housed in an IP54 enclosure accommodating the internal optical fibre layout and all user-facing external components as shown in Fig. 3b. The total power consumption of each station is less than 40 mW electrical power provided by 120 mW optical power.

3.2 Remote terminal unit (RTU)

The RTU is the heart of the whole system: it normally sits in the air-conditioned room, connects and sends light to each gas monitoring station while collecting all the information of interests to the end users. It is intentionally structured, with light source module sending light to each station, photodetector module converting the received optical signal back to electrical signal, and data acquisition (DAQ) module decoding the electrical signal into presentable format for webpage display and data storage (see Fig. 4). All modules share a 12 V DC supply and the whole RTU consumes less than 18 W. For a system with two gas monitoring stations, two light source modules are installed each dedicated to one station.

3.2.1 Light source module

We choose 1550 nm wavelength light and SMF for the system as they are commonly used in telecommunication with corresponding mature and inexpensive optical components. And as many industries already have optical communication networks in place, an SMF system offers a high degree of compatibility.

The light source is used both for powering and signal transmission. To power each station, at least 110 mW optical power is required; and for signal transmission, we need broad-band light with low noise at relatively low frequency (under 10 kHz) for sensing purpose. In addition, a protection circuit for overpower protection is required for intrinsic safety. To the best of our knowledge, no light source on the market can serve all these purposes, so we manufactured the light source, which was designed to be compact, reliable, powerful and, importantly intrinsically safe.

3.2.2 Photodetector module

The photodetector module converts the optical signal into an electrical signal, then cleans and amplifies it. It also provides display and controls for user to both monitor and adjust the output voltage. The module is designed to measure up to 4 optical channels. They are powered by 12 V DC and draw around 170 mA of current. The intensity of the light from each optical input port is measured by a dedicated InGaAs photodiode and converted into a current. The DC and AC components of this current are separated and converted into voltages. The DC voltage represents the background light reflected back from the optical transducer and the AC voltage represents the signal carrying the digital information

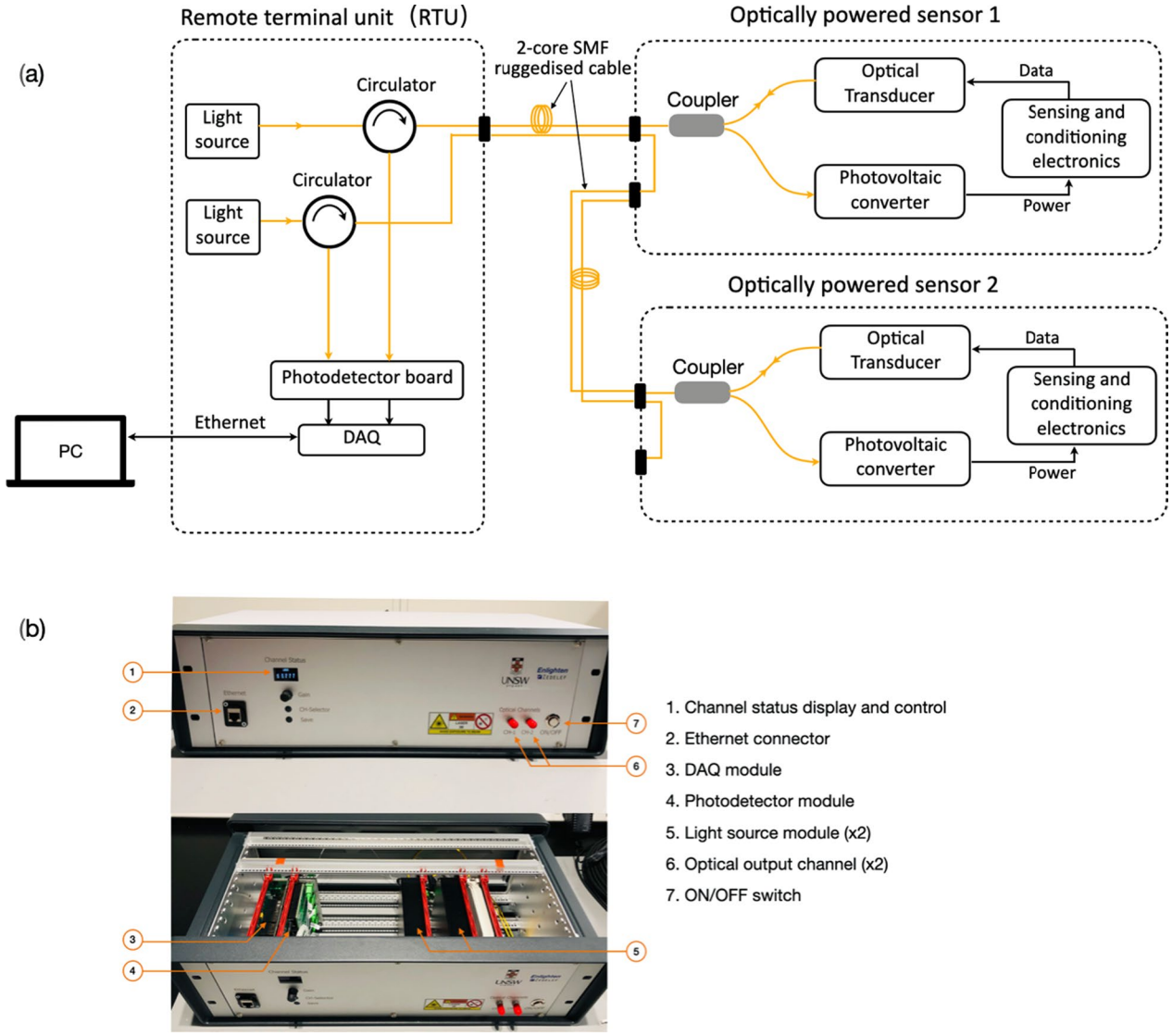

Fig. 4 RTU block diagram and its connection with two optically powered sensors (in daisy-chain configuration) and RTU and its constitutive modules

of interest. The AC voltage of each channel is coupled to a driving amplifier and the gain can be adjusted on the front panel to a level suitable for DAQ module.

3.2.3 DAQ module

The DAQ module is designed to decode and process the signal from the photodetector module. It is also powered 12 V DC and draws around 200 mA current. It supports an Ethernet interface and data logging. The information each sensor—in the form of 8 Manchester packets—are read and logged to volatile SDRAM memory every second and given a timestamp. The real-time data of each sensor includes: ID of gas monitoring stations, gas concentrations of CH_4, CO, CO_2 and O_2, Ambient temperature, ambient barometric pressure, operation modes, optical power level, and battery level.

These data with timestamps can be shown graphically on a standard web browser on a PC or mobile device via an Ethernet interface. Every minute, the information of each station is logged in the µSD card on the DAQ board with timestamps. Data logs can be downloaded as.csv files from the home webpage.

3.3 Daisy chain configuration

Two topologies are supported in this optical network. Each station can connect to the RTU separately (star topology) or in a daisy-chained connection with other stations. For the daisy-chained network, N-core optical cables are needed for

a system of N gas monitoring stations. As shown in Fig. 3b, each station has two optical ports—'Light in' and 'Light out'. Light comes in from 'Light in' port and drops one optical core dedicated to one station while the other cores go on to 'Light out' port to be connected to the next station's 'Light in' port. The daisy chain network saves cabling from the RTU and increases distance coverage. In our two-station system, the daisy chain configuration illustrated in Fig. 4 a shows that with the same lengths of cables, the chained device extends the coverage while still enjoys the dedicated SMF for power and data transmission. The complete system ready for field trial with two gas monitoring stations daisy-chained by two 2-core 100-m long ruggedised optical cables is shown in Fig. 5.

4 Field trials and results

Filed trials have been carried out at BMA's Broadmeadow underground coal mine. The system shown in Fig. 5 was explained in detail and demonstrated on the surface to technical mining engineers before its formal installation on site. Engineers were able to try the operation of the system according to the user manual and got ready for the installation.

4.1 Installation

The system was installed at two distinct locations: the two gas monitoring stations were installed side-by-side underground about 150 m below the surface and the RTU on the surface in an air-conditioned, on-site communication room (a.k.a. Comms Hut). In the Comms Hut, the RTU's optical output channels were connected to two cores of a 250-m-long optical fibre cable running from the surface to an underground location (a.k.a. cut-through) into the marshalling cabinet and breakout box where the two cores were further connected to the ruggedised optical cable to power the two stations. The optical network configuration and installation of the system are illustrated in Fig. 6.

4.2 Results and data analysis

The data collected covers the period from 17/12/2020 (at 13:04) to 14/02/2021 (09:48), in other words 59 days or 1413 consecutive hours. For the entire duration of the field trials, both monitoring stations were placed side-by-side in a relatively clean environment (see Fig. 6b) and reported consistent data for all measured quantities.

All data presented below was acquired in the Broadmeadow control room sitting on the surface and connected to RTU via Ethernet. Figure 7 highlights a screen grab of the data acquired during the very first day of deployment.

4.2.1 Temperature and pressure

Figure 8 illustrates the ambient temperature dependence as monitored during the whole field trial period. It clearly demonstrates the change in temperature from diurnal to nocturnal periods and a high degree of agreement between the two monitoring stations. This last statement can be quantified by looking at the standard deviation of the difference in temperature reported by the two stations over

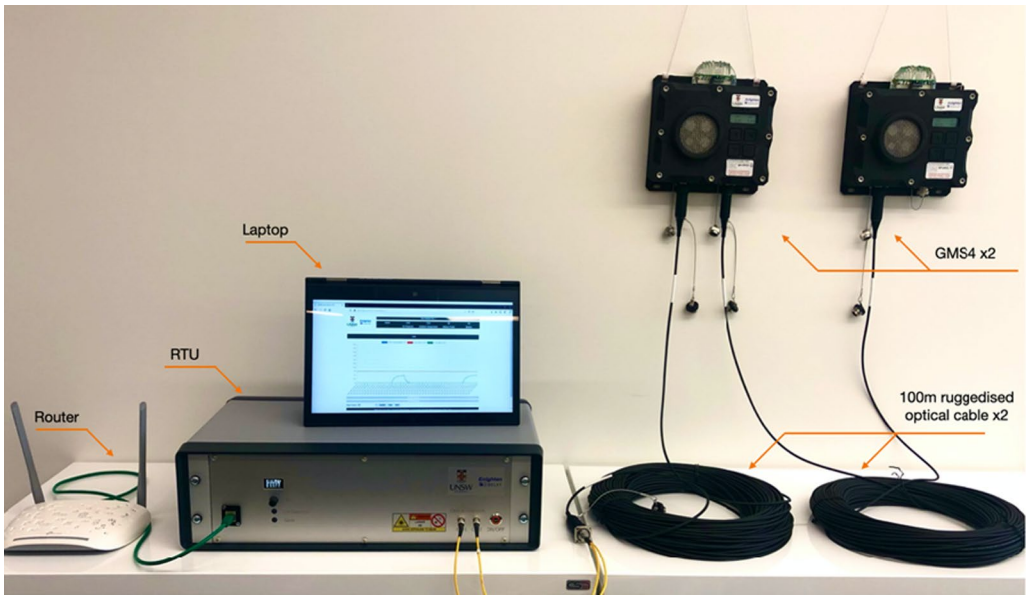

Fig. 5 Certified intrinsically safe, optically powered gas monitoring system with daisy-chained topology

Fig. 6 Installation of the system at Broadmeadow mine. **a** RTU is installed on the surface at the Comms hut connecting to the mine's optical fibre network. **b** Two gas monitoring stations installed 150 m underground for environmental gas detection

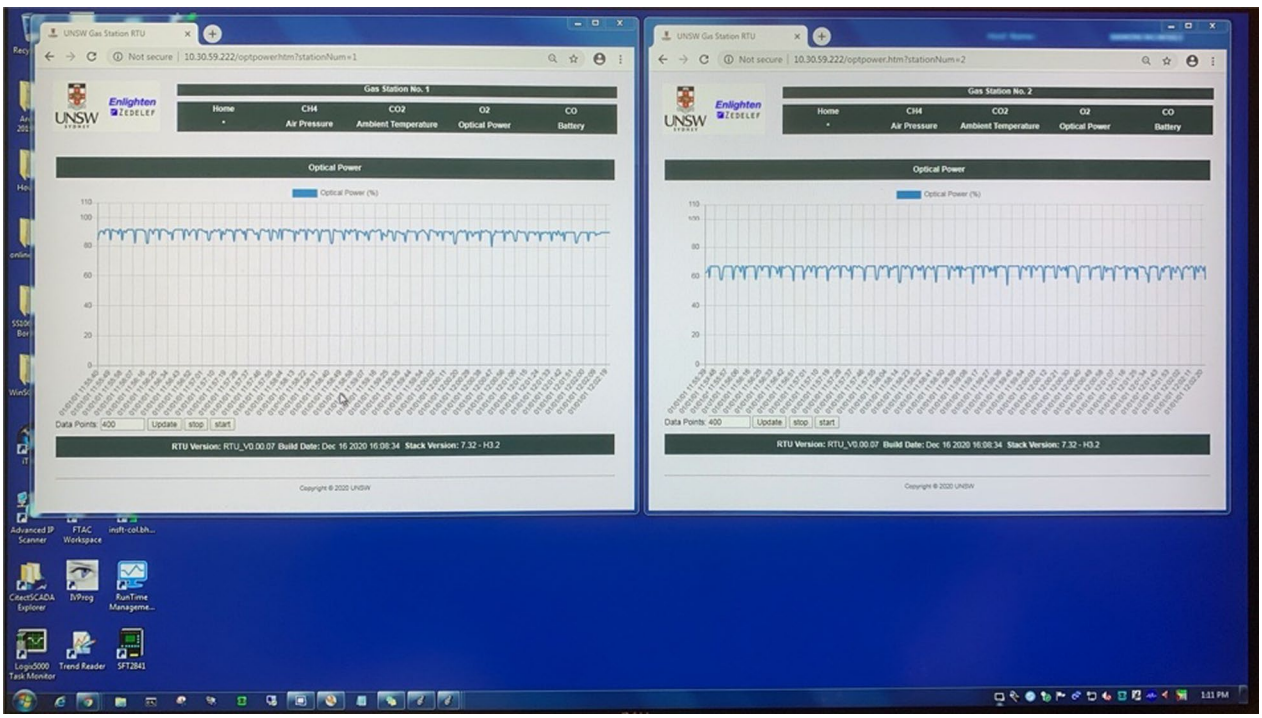

Fig. 7 Screen grab of the data reported by both gas monitoring stations during their first day of operation. As shown, the data (optical power delivered to both stations) covers a time scale of about 6 min

the sampling period which amounts to 0.016 °C, in good agreement with the nominal accuracy of the temperature sensor (0.01 °C).

Likewise, Fig. 9 illustrates the ambient pressure at the sensors' location. Again, we see excellent agreement tween the two monitoring stations over the whole data collection period. The standard deviation of the difference pressure reported by both sensors over the sampling period is 0.062 hPa, well within the reported accuracy of the sensor reported as ± 0.12 hPa.

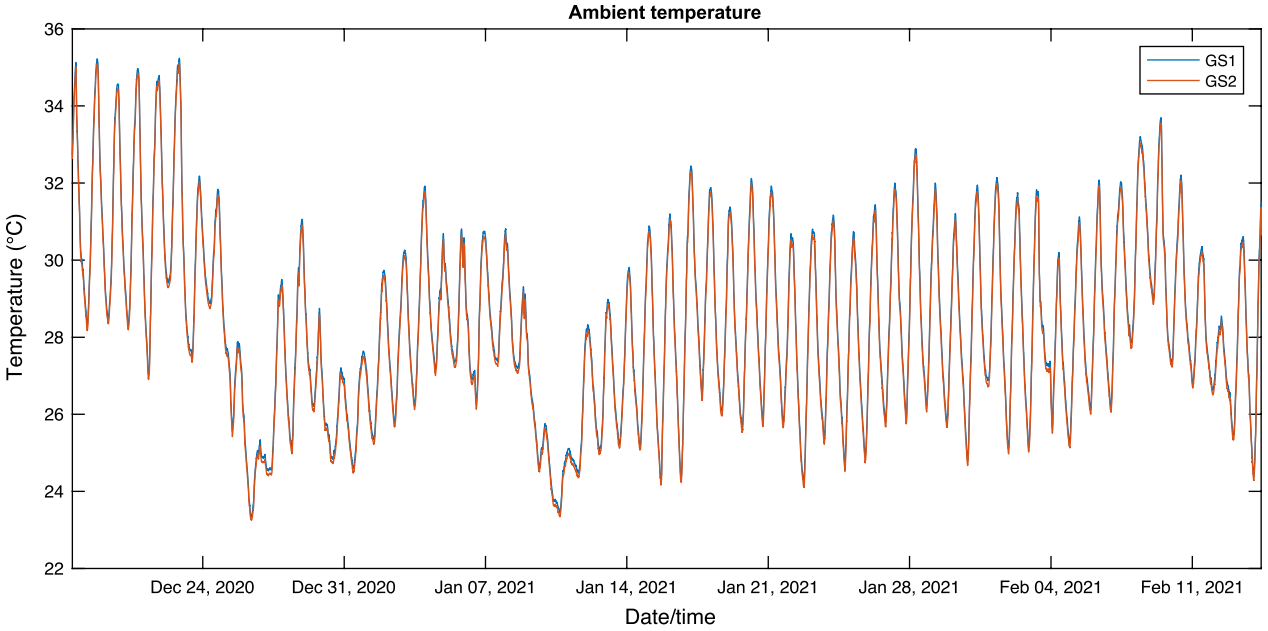

Fig. 8 Ambient temperature as reported by the two gas monitoring stations (GS1 and GS2). Note the cyclical 24 h periodicity due to day-night transition. On average 28.4 ± 2.4 °C for GS1 and 28.2 ± 2.4 °C for GS2

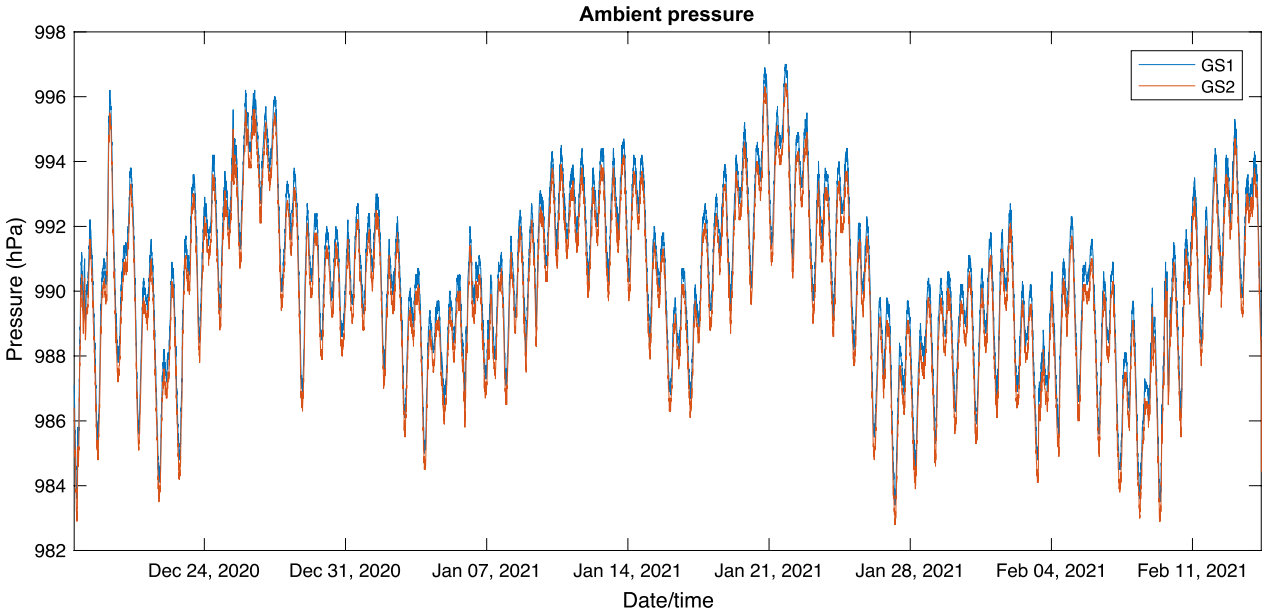

Fig. 9 Ambient pressure as reported by the two gas monitoring stations (GS1 and GS2). Again, note the cyclical 24 h periodicity due to day-night transition. On average 990.6 ± 2.5 hPa for GS1 and 990.0 ± 2.5 hPa for GS2

4.2.2 Gas sensing

As mentioned, the monitoring capabilities of the stations include CO, CO_2, CH_4 and O_2. Under the conditions of the test, and except for oxygen, all gas levels are essentially zero and are within the noise of the respective sensors. Figure 10 illustrates the levels of O_2 as reported by both stations. The plotting scale clearly highlights the digital nature of the data as reported to the RTU on a quantified grid using integer multiple of 0.1%. Again, we note the excellent agreement between both stations; in fact, calculating the standard deviation of the difference in concentration reported by both stations yields 0.070%.

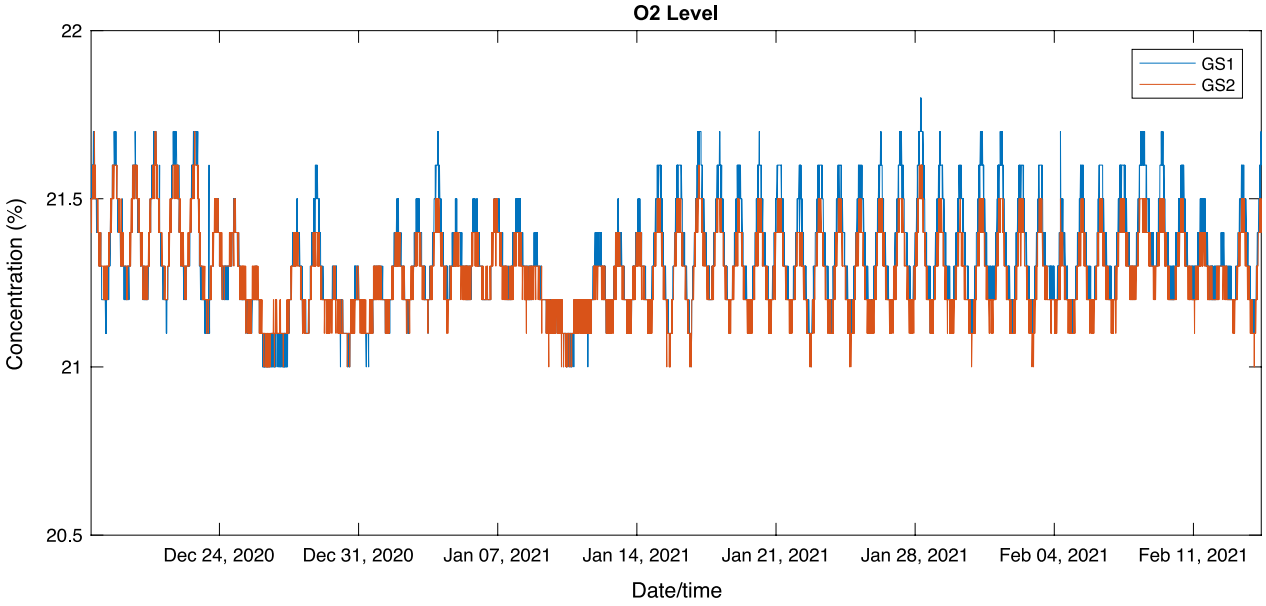

Fig. 10 Oxygen levels as report by both stations with an average of 21.3% ± 0.2% for GS1 and 21.3% ± 0.1% for GS2

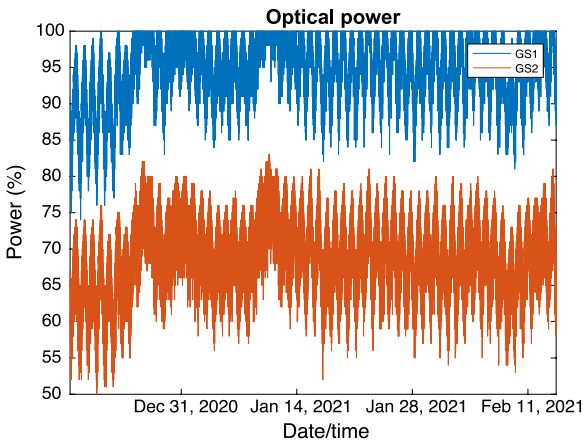

Fig. 11 Optical power received by both gas monitoring stations. When expressed in percentage, we have for GS1 96.8% ± 3.9% and 72.1% ± 4.9% for GS2

4.2.3 Optical power and battery levels

It is instructive to analyse the optical power received by the gas monitoring stations as a function of time. Figure 11 illustrates this for both gas stations.

The optical power is reported based on a measurement of the voltage at the photovoltaic converter pins and to give an idea of relative levels, a reported 100% corresponds to 3.7 V as upper limit and 0% is 3 V hence the clipping exhibited by GS1 in Fig. 11, where the output voltage under load goes above its typical maximum value. We next note that the GS1 receives more optical power that GS2 which is understandable given the fact that the stations are daisy-chained and GS1 is located closer to the optical source than is GS2. The difference in power can thus be accounted for by (1) an additional 100 m of optical path and (2) an additional number of optical connectors.

As explained, both gas stations contain a battery used during alarm and in case of a sudden, unplanned optical power outage. Under normal circumstances, which is precisely the conditions under which the stations have been operating, the battery level should remain unchanged. Figure 12 illustrates an issue related to the battery level of GS1 which is clearly and steadily degrading in time.

A closer analysis shows that between 02:00 and 08:00 on December 25th some anomalous behaviour started. Before that period, the battery for both stations were reported as 100% capacity. After 08:00, the battery level of GS1 started to degrade. At the time of this writing, the reason for this behaviour is unknown but due to its sudden appearance on December 25th, this is probably due to a firmware fault. This will be investigated upon the recall of the stations.

5 Conclusions

The current project aimed at delivering a fully functional, intrinsically safe, ruggedised optically powered gas sensing network and we have detailed herein the path taken to achieve this goal. Doing so, we have demonstrated the viability of PoF technology for intrinsically safe, multi-gas monitoring station over long distance.

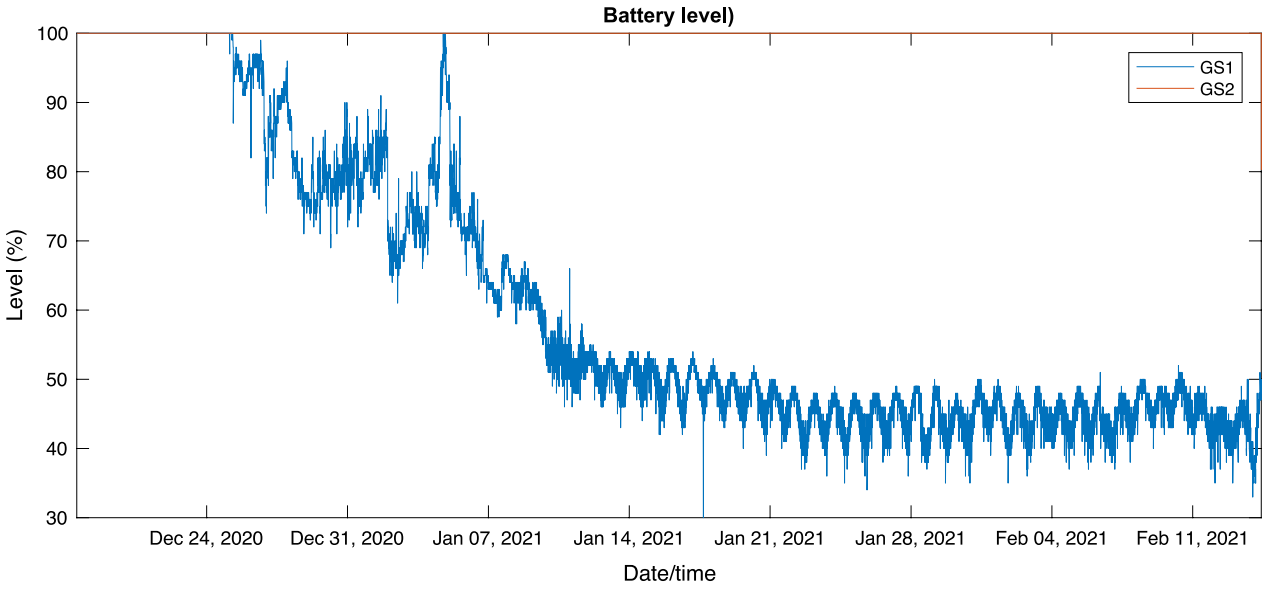

Fig. 12 Battery levels are reported by both gas monitoring stations. Note how GS2 reports constant battery level of 100% while GS1 start degrading around December 25th despite receiving more optical power that GS2

The field trials have also successfully proven that the technology can be deployed under real-life conditions. Furthermore, the network remained in operation for almost 60 days uninterrupted and both stations reported cross-validated data (i.e. data sets in agreement with each other).

Lastly, future potential commercial implementation will of course need to include a number of improvements, either suggested by the on-going interactions with end users or following from the lessons learnt during the field trials. These improvements should include:

(1) Software improvements: The next iteration of a more mature UI/UX targeting integration into the end-user supervisory control and data acquisition (SCADA) system.
(2) Hardware improvements: a redesign of the gas monitoring station and accompanying remote terminal unit to incorporate improvements derived from a better understanding of the requirements as shown during the field trials. For example, replacing battery with supercapacitor, improved visibility of displays, enclosures designed for scale production, etc.

Acknowledgements The authors kindly acknowledge the financial support of the Australian Coal Industry's Research Program (ACARP Grant C28010).

References

AS/NZS 2290.3 (2018) Electrical equipment for coal mines—introduction, inspection and maintenance. Part 3: gas detecting and monitoring equipment. Standard, Electrical Equipment in Mines and Quarries

Bassan FR, Rosolem JB, Floridia C et al (2021) Power-over-fiber LPIT for voltage and current measurements in the medium voltage distribution networks. Sensors 21:547. https://doi.org/10.3390/s21020547

Brodzeli Z, Silvestri L, Michie A et al (2013a) Reflective mode of deformed helix ferroelectric liquid crystal cells for sensing applications. Liq Cryst 40:1427–1435. https://doi.org/10.1080/02678292.2013.807942

Brodzeli Z, Silvestri L, Michie A et al (2013b) Sensors at your fibre tips: a novel liquid crystal-based photonic transducer for sensing systems. J Lightwave Technol 31:2940–2946. https://doi.org/10.1109/JLT.2013.2274455

Budelmann C (2018) Opto-electronic sensor network powered over fiber for harsh industrial applications. IEEE Trans Ind Electron 65:1170–1177. https://doi.org/10.1109/TIE.2017.2733479

DeLoach BC Jr, Miller RC, Kaufman S (1978) Sound alerter powered over an optical fiber. Bell Syst Tech J 57:3309–3316

Dubaniewicz TH Jr, Chilton JE (1995) Optically powered remote gas monitor. Report, U.S. Department of the Interior. Report of Investigations

Einicke G, Hainsworth D, Munday L et al (2011) Optically-powered underground coal mine communications. In: Coal Operators' Conference, Mining Engineering, University of Wollongong. https://ro.uow.edu.au/coal/358

Firth J, Ladouceur F, Brodzeli Z et al (2016) A novel optical telemetry system applied to flowmeter networks. Flow Meas Instrum 48:15–19. https://doi.org/10.1016/j.flowmeasinst.2016.01.006

Firth J, Ladouceur F, Brodzeli Z et al (2017) Liquid crystal based optical telemetry applied to 4–20 ma current loop networks. Sens Actuators A260:124–130. https://doi.org/10.1016/j.sna.2017.04.005

Heinig S, Jacobs K, Norrga S et al (2020) Single-fiber combined optical power and data transmission for high-voltage applications. In: The 46th annual conference of the IEEE Industrial Electronics Society, IECON, Singapore

IEC 60079-0 (2017) Explosive atmospheres—part0: equipment—general requirements. International standard, International Electrotechnical Commission

IEC 60079-11 (2011) Explosive atmospheres—part 11: equipment protection by intrinsic safety "i". International standard, International Electrotechnical Commission

IEC 60079-28 (2015) Explosive atmospheres—part28: protection of equipment and transmission systems using optical radiation. International standard, International Electrotechnical Commission

Lei XY, Wieschendorf C, Hao L et al (2020) Compact actively Q-switched laser for sensing applications. Measurement 173:108631. https://doi.org/10.1016/j.measurement.2020.108631

López-Cardona JD, Vázqueza C, Montero DS et al (2018) Remote optical powering using fiber optics in hazardous environments. J Lightwave Technol 36:748–754. https://doi.org/10.1109/JLT.2017.2776399

Palchik V (2014) Time-dependent methane emission from vertical prospecting boreholes drilled to abandoned mine workings at a shallow depth. Int J Rock Mech Min Sci 72:1–7. https://doi.org/10.1016/j.ijrmms.2014.08.002

Rosolem JB (2017) Power-over-fiber applications for telecommunications and for electric utilities. Roka R (ed). InTech, London

U.S. Environmental Protection Agency (2014) Methane emissions from abandoned coal mines in the United States. United States: EPA 430-R-04-001

Vázquez C, López-Cardona JD, Lallana PC et al (2019) Multicore fiber scenarios supporting power over fiber in radio over fiber systems. IEEE Access 7:158409–158418. https://doi.org/10.1109/ACCESS.2019.2950599

Wake D, Nkansah A, Gomes NJ et al (2008) Optically powered remote units for radio-over-fiber systems. J Lightwave Technol 26:2482–2491. https://doi.org/10.1109/JLT.2008.927171

Wasilewski S, Jamóz P (2018) Distribution of methane concentration in the ventilating area of the longwall. J Min Sci 54(6):1004–1013. https://doi.org/10.1134/S1062739118065167

Werthen JG, Widjaja S, Wu TC, Liu J (2005) Power over fiber: a review of replacing copper by fiber in critical applications. Proc SPIE. https://doi.org/10.1117/12.619753

Xu X, Yang SG, Zhang C et al (2010) Optically powered communication system with distributed amplifiers. J Lightwave Technol 28(21):3062–3069. https://doi.org/10.1109/JLT.2010.2076346